Temperature and strain-rate dependent fracture strength of graphene

H. Zhao and N. R. Aluru[a)]
Department of Mechanical Science and Engineering, Beckman Institute for Advanced Science and Technology, University of Illinois at Urbana–Champaign, Urbana, Illinois 61801, USA

(Received 29 June 2010; accepted 7 August 2010; published online 22 September 2010)

We investigate the variation in fracture strength of graphene with temperature, strain rate, and crack length using molecular dynamics (MD) simulations, kinetic analysis of fracture with a nonlinear elastic relation, and the quantized fracture mechanics theory. Young's modulus does not vary significantly with temperature until about 1200 K, beyond which the material becomes softer. Temperature plays a more important role in determining the fracture strength of graphene. Our studies suggest that graphene can be a strong material even, when subjected to variations in temperature, strain rate, and cracks. © *2010 American Institute of Physics*. [doi:10.1063/1.3488620]

I. INTRODUCTION

The observation of novel properties at nanoscale, including material properties, has intensified the design and development of nanoelectromechanical-systems (NEMS) for various applications. A significant number of studies have been performed on one-dimensional nanostructures, such as nanowires and nanotubes, to understand their mechanical, electrical, thermal, and optical properties at nanoscale. The mechanical properties of nanostructures, especially their stiffness and strength, need to be carefully understood as they can be the key factors in determining the stability and lifetime of many potential NEMS applications. Extensive experimental and numerical simulations have been performed to understand mechanical properties of nanostructures including carbon nanotube (CNT),[1,2] silicon nanotube (SiNT),[3] GaN nanotube (GaNNT),[4] silicon carbide (β-SiC) nanowire,[5,6] silicon nitride (α-Si_3N_4) nanowire,[7] Gold nanowire,[8,9] Pd–Pt nanowire,[10] and glass silica nanowire.[11] The ultimate strength of these nanostructures have been measured or calculated to be 11–83 GPa for CNT, 7–10 GPa for SiNT, 18–66 GPa for GaNNT, 17–110 GPa for β-SiC, 17–59 GPa for α-Si_3N_4, 2–8 GPa for gold nanowires, 8–18 GPa for Pd–Pt nanowires and 9–26 GPa for glass silica nanowires. The variation in the strength mainly depends on the critical size (e.g., diameter), temperature and strain rate. Temperature and strain rate have been shown to play an important role in determining the tensile strength and tensile strain of the CNTs.[12] Pristine nanostructures are somewhat difficult to fabricate at the nanoscale and defects can play an important role in significantly altering the strength of the nanostructure. For example, the tensile strength of CNTs can be reduced to 60% of the pristine tube value if vacancies are present.[13] The crack length is more important compared to the crack shape in determining the tensile strength of defective CNTs.[14] All these studies and results indicate that temperature and defects can play an important role in determining the tensile strength of one-dimensional nanostructures.

Ever since graphene was first observed,[15] several studies have shown that graphene is a stable two-dimensional lattice with exceptional electronic and optical properties.[16,17] Recent experiments have shown graphene to be the strongest material currently known[18] with fracture strength of 130 ± 10 GPa at room temperature and stiffness as high as 1 TPa. The excellent mechanical, electrical and optical properties of graphene makes graphene a promising two-dimensional material for NEMS and other applications. As a result, it is important to more clearly understand and accurately estimate the strength and stiffness of graphene under various conditions. Using *ab inito* calculations, the tensile strength of graphene under uniaxial tension has been shown to depend strongly on the chirality of graphene with the maximum Cauchy stress of 110 GPa in the armchair direction and 121 GPa in the zigzag direction.[19] Using classical molecular dynamics (MD) simulations, the Young's modulus of graphene nanoribbons has been shown to increase with size of the nanoribbon and approach 1 TPa for bulk graphene.[20] The variation in the tensile strength of graphene with crack length for uniaxial tension in the armchair direction has also been studied and compared with the classical fracture mechanics theory.[21]

To further accelerate the design and development of graphene-based nanodevices, in this paper, we perform systematic studies to understand the dependence of fracture strength of graphene monolayer on temperature, strain rate and crack length. We develop a theoretical framework for fracture strength and fracture strain as a function of temperature and strain rate for the pristine monolayer graphene based on the kinetic analysis of fracture. We further use the quantized fracture mechanics (QFM) theory to predict the relation between fracture strength and crack length of graphene. The theoretical predictions have been compared with classical MD simulations. The rest of the paper is organized as follows. In Sec. II, we introduce the basic concepts and discuss kinetic analysis of fracture. In Sec. III, we briefly introduce the QFM theory. Results and discussion on the variation in fracture strength with temperature, strain rate and cracks are given in Sec. IV. Comparison between numerical results and theory is also presented in Sec. IV and conclusions are given in Sec. V.

[a)]Electronic mail:aluru@illinois.edu.

II. KINETIC ANALYSIS OF FRACTURE

Systematic experimental investigations have shown that stress and temperature are two dominant factors that determine the lifetime of a loaded solid.[22] In the thermal activation theory of Eyring,[23] the Arrhenius formula[24] relates the lifetime τ as a function of tensile stress σ and temperature T by the expression[12]

$$\tau = \frac{\tau_0}{n_s}\exp\left(\frac{U_0 - \gamma\sigma}{kT}\right), \tag{1}$$

where τ_0/n_s is the pre-exponential factor, τ_0 is the vibration period of atoms in solid, n_s is defined as the number of sites available for the state transition, U_0 is the interatomic bond dissociation energy, and $\gamma=qV$, where V is the activation volume and q is the coefficient of local overstress, and k is the Boltzmann constant. The lifetime τ, defined as the time taken for a stressed solid to breakdown, is directly related to the energy barrier $U_0-\gamma\sigma$ and the temperature T, by the Maxwell–Boltzmann distribution. The energy barrier is typically lowered by the applied tensile stress and the thermal motion of atoms can also overcome the energy barrier and result in bond dissociations.

In the uniaxial tensile test, when the tensile stress varies with time, i.e., if $\sigma=\sigma(t)$, the rule of partial lifetime summation leads to the Bailey's principle,[25] which states that the fracture is initiated when

$$\int_0^{t_r} \frac{dt}{\tau[T,\sigma(t)]} = 1, \tag{2}$$

where t_r is the time to failure. The fracture strength σ_r is defined as the stress in the structure when breakdown occurs. With constant strain rate, $\sigma(t)$ is directly related to the constitutive relation of the material.

For a linear elastic (LE) material, with Young's modulus K, σ, and σ_r can be defined as

$$\sigma(t) = K\epsilon(t) = K\dot{\epsilon}t, \quad \sigma_r = K\dot{\epsilon}t_r. \tag{3}$$

Substituting Eqs. (1) and (3) into Eq. (2), we have

$$\sigma_r(\dot{\epsilon},T) = \frac{U_0}{\gamma} + \frac{k}{\gamma}\ln\left(\frac{\gamma K\dot{\epsilon}\tau_0}{n_s kT}\right)T, \tag{4}$$

which shows the linear relation between fracture strength and temperature, where $\ln(\gamma K\dot{\epsilon}\tau_0/n_s kT)$ can be considered as a constant.[12,26] The corresponding fracture strain ϵ_r and the transition time t_r can be obtained as

$$\epsilon_r = \frac{\sigma_r}{K}, \tag{5}$$

$$t_r = \frac{\sigma_r}{K\dot{\epsilon}}. \tag{6}$$

Graphene has been shown to exhibit nonlinear elastic (NLE) behavior under uniaxial tension.[19,20] In order to develop an explicit analytical expression for σ_r, we define $\sigma(t)$ under constant strain rate using two parameters a and b as

$$\sigma(t) = a\,\ln[b\epsilon(t) + 1.0] = a\,\ln[b\dot{\epsilon}t + 1.0]. \tag{7}$$

Thus, σ_r can be defined as $\sigma_r=a\,\ln[b\dot{\epsilon}t_r+1.0]$. Substituting Eq. (7) and Eq. (1) into Eq. (2), we have

$$\sigma_r(\dot{\epsilon},T) = \frac{akT}{\gamma a + kT}\left\{\frac{U_0}{kT} + \ln\left[\frac{b\dot{\epsilon}\tau_0}{n_s}\left(\frac{\gamma a}{kT}+1\right)\right]\right\}. \tag{8}$$

The fracture strain and the transition time are defined as

$$\epsilon_r = \frac{1}{b}\left[\exp\left(\frac{\sigma_r}{a}\right) - 1.0\right], \tag{9}$$

$$t_r = \frac{1}{b\dot{\epsilon}}\left[\exp\left(\frac{\sigma_r}{a}\right) - 1.0\right]. \tag{10}$$

When $b\to 0$, the NLE relation given in Eq. (7) can be shown to reduce to the LE relation $\sigma\approx ab\epsilon$ using the Taylor series expansion and neglecting the second and higher order terms. The corresponding fracture properties, Eqs. (8)–(10), will reduce to the expressions given in Eqs. (4)–(6). Thus, with the kinetic analysis of fracture, analytical expressions relating the fracture strength under uniaxial tensile test as a function of temperature and strain rate can be developed.

III. QUANTIZED FRACTURE MECHANICS

In the LE fracture mechanics theory, the well established Griffith's[27] criterion implies that a crack can form or grow only if the process causes the total energy to decrease or remain constant. When the variation in the total potential energy dW, corresponding to a virtual increment of the crack surface dA, becomes equal to the energy spent to create the new free crack surface, i.e., $dW+G_c dA=0$, the crack will propagate, where G_c is the fracture energy. However, in nanoscale, the crack propagates in a discrete manner, whenever one interatomic bond is broken. Recently, a new energy-based QFM (Refs. 28 and 29) theory has been formulated by substituting the differentials in Griffith's energy balance with finite differences, in order to take into account the underlying crystal structure. Under mode I loading, a blunt crack on a finite width plate is considered in our study. The plate width is defined as $2w$, the crack length is defined as $2L$ and the tip radius of the crack is defined as ρ. The fracture strength using QFM is given by[28,30]

$$\sigma_f(L) = \sigma_r(\dot{\epsilon},T)\sqrt{\frac{1+\rho/2L_0}{1+2L/L_0}}\left[\frac{2w}{\pi L}\tan\left(\frac{\pi L}{2w}\right)\right]^{1/2}, \tag{11}$$

where σ_r is the fracture strength of the defect-free lattice, $2w$ is the finite width of the plate, and L_0 is the fracture quantum defined as the minimum crack extension corresponding to the breaking of one interatomic bond along the crack direction. For the defect-free structure, as $L=0$ and $\rho=0$, Eq. (11) can be simplified as $\sigma_f(0)=\sigma_r$.

Even though QFM theory is based on discrete crack propagation, it assumes that the medium is linear and elastic. For NLE behavior, corrections[29] have been reported. However, when fracture occurs in the LE region due to the slit cracks, the corrections can be neglected. Thus, Eqs. (8) and (11) serve as the theoretical approximations of the fracture

strength of graphene monolayer as a function of temperature, strain rate, crack length, crack tip radius, and the defect density.

IV. RESULTS AND DISCUSSION

A. Pristine graphene

In order to investigate the mechanical properties of graphene under various temperatures and loading conditions, MD simulations are performed using LAMMPS (Ref. 31) with the adaptive intermolecular reactive empirical bond order (AIREBO) potential.[32] AIREBO potential has been shown to accurately capture the Young's modulus of graphene[20] as well as bond breaking and bond reforming between carbon atoms. The cutoff parameter is set to be 2.0 Å in order to avoid the spuriously high bond forces and nonphysical results near the fracture region.[33] In our previous study,[20] we have shown that the fracture strength and fracture strain of monolayer graphene under tension are larger in the zigzag direction compared to that of in the armchair direction. In this study, we only investigate the uniaxial tensile test of graphene along the armchair direction. To investigate the Young's modulus and fracture properties, we perform calculations on a 100.8 Å × 102.2 Å size pristine graphene monolayer (3936 atoms) with periodic boundary condition along the in-plane two directions. This size is large enough to represent the mechanical properties of an infinitely large graphene monolayer. Starting with a uniformly distributed initial velocity profile, we perform Isothermal-Isobaric (NPT) simulations at the specified temperature for 200 ps with a time step of 0.1 fs to let the system reach its equilibrium configuration. Then, we perform deformation-controlled uniaxial tensile test along the armchair direction of the structure by applying the strain rate of 0.001 ps^{-1}. The pressure component perpendicular to the loading direction is controlled to maintain the uniaxial tensile condition. The strain increment is applied to the structure after every one time step with the step size of 0.1 fs. For each temperature, we run two or three independent loading tests by adopting different initial configurations. The nominal strain, nominal stress and Young's modulus are calculated the same way as described in Ref. 20.

The stress-strain relations for various temperatures ranging between 300 K and 2400 K are shown in Fig. 1(A). As shown in the figure, a NLE behavior is observed for graphene. The fracture strength and fracture strain decrease significantly with the increase in temperature. As shown in Fig. 1(B), the Young's modulus exhibits minor variation with temperature till around 1200 K. Beyond that, the Young's modulus decreases and the material become softer with the increase in temperature. Even at high temperature, e.g., at 2400 K, the Young's modulus of graphene is 0.9 TPa, which is approximately 10% lower compared to the room temperature value. This suggests that graphene, when compared to other materials, can be a strong material even at higher temperatures. The fracture strength of graphene decreases with the increase in temperature. The fracture strength at 2400 K is about 60% lower compared to that at room temperature. Figure 2 shows the variation in tensile strength of graphene

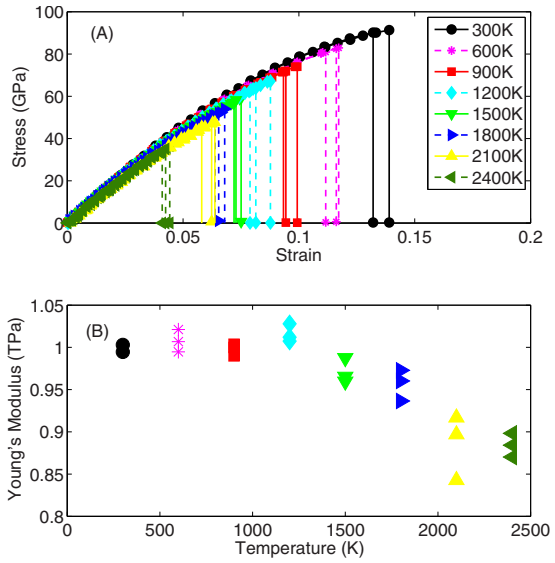

FIG. 1. (Color online) (A) Nominal strain vs stress of graphene under uniaxial tensile test along the armchair direction at various temperatures. (B) Variation in Young's modulus of graphene with temperature under uniaxial tensile test along the armchair direction.

with temperature. Comparison is also presented with experimental and numerical data reported in literature for CNT, SiNT, GaNNT, silicon carbide nanowire, silicon nitride nanowire, gold nanowire, Pd–Pt nanowire, and glass silica nanowire. The comparison indicates that graphene, a two-dimensional nanomaterial, is one of the strongest material known to date.[18]

In order to check the accuracy of the theoretical approximations for fracture strength [Eq. (8)], fracture strain [Eq. (9)], and transition time [Eq. (10)] with the NLE constitutive relation, we use $\tau_0 = 10^{-13}$ s (Ref. 22) as the average vibration period of atoms in solid. With the AIREBO potential, the bonding energy and the activation volume show a negligible variation with temperature. Accordingly, we define

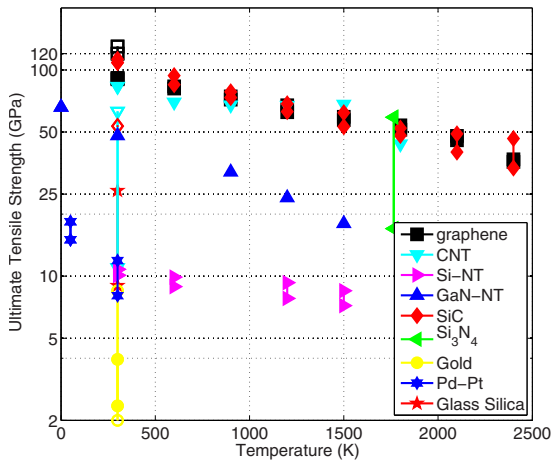

FIG. 2. (Color online) Comparison of the ultimate tensile strength σ_r of graphene at various temperatures with values reported in the literature for CNT (Refs. 1 and 2), SiNT (Ref. 3), gallium nitride nanotube (Ref. 4), silicon carbide (β-SiC) nanowire (Refs. 5 and 6), silicon nitride (α-Si_3N_4) nanowire (Ref. 7), gold nanowire (Refs. 8 and 9), Pd–Pt nanowire (Ref. 10), and glass silica nanowire (Ref. 11). The filled symbols are numerical simulation results and the corresponding hollow symbols are the experimental data.

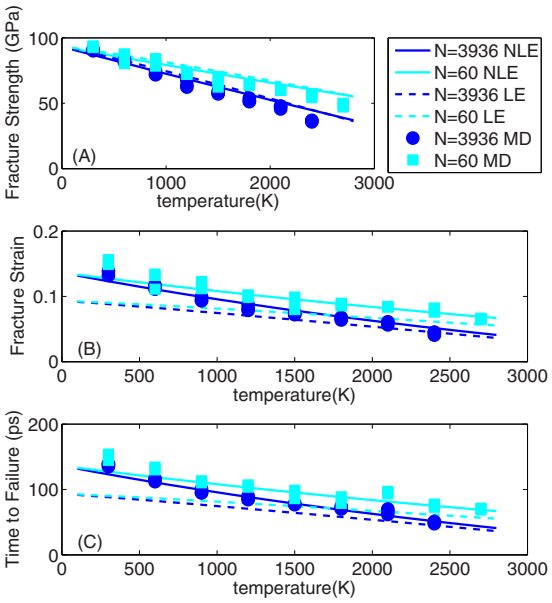

FIG. 3. (Color online) Variation in the fracture strength, fracture strain, and transition time as a function of temperature for two different system sizes (60 atoms and 3936 atoms). The symbols are from MD simulations. The lines are from the theoretical approximations [Eqs. (8)–(10)].

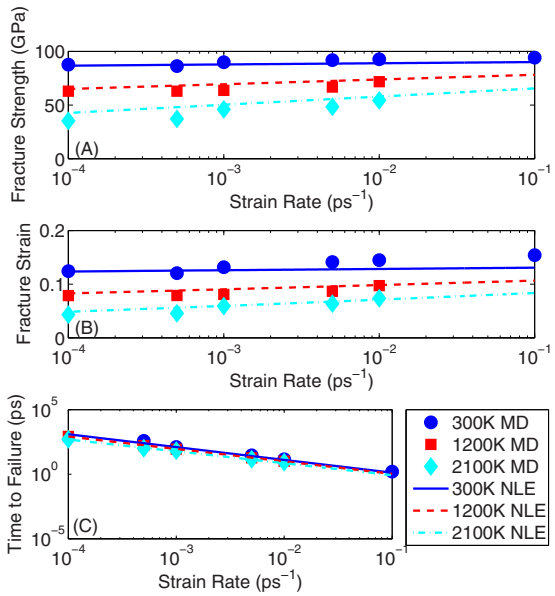

FIG. 4. (Color online) Variation in the fracture strength, fracture strain, and transition time as a function of strain rate for three different temperatures (300, 1200, and 2100 K). The symbols are from MD simulations. The lines are from the theoretical approximations [Eqs. (8)–(10)].

U_0=4.94 eV and γ=8.49 Å^3, with the assumption of q=1. Since the strain-stress relation has a minor variation with temperature, using the least-squares technique, we calculate $a=1.11\times10^{11}$ Pa and b=9.69 for the NLE behavior given in [Eq. (7)]. For the LE behavior [Eq. (3)], we use K=1.0 TPa. $n_s=1.5N$ is defined as the total number of bonds that can be broken in an N atom system.

Considering two different sizes of the graphene lattice, a small size of N=60 and a large size of N=3936, we investigate the variation in the fracture properties with temperature. In MD simulations, the strain rate and time step are defined as 0.001 ps^{-1} and 0.1 fs, respectively. Figure 3 shows the variation in the fracture strength, fracture strain, and transition time as a function of temperature for the two different system sizes. MD simulation results and the theoretical approximations with both the LE model and NLE model are presented. Clearly, temperature plays an important role as it reduces the fracture strength and fracture strain. The LE theoretical model does not accurately estimate the variation in the fracture strain and transition time with temperature. The NLE theoretical model provides a good estimate of all the fracture properties as the results match reasonably well with the MD simulation results.

For the N=3936 system, we further investigate the variation in the fracture properties with strain rate at temperatures of 300, 1200, and 2100 K. Figure 4 shows the variation in the fracture properties with strain rate at different temperatures. The comparison between MD results (symbols) and NLE theoretical model (lines) are presented. Both the fracture strength and the fracture strain decrease slightly with the decrease in the strain rate at low temperature (300 K) but the strain rate effect is more prominent at high temperature (2100 K). Compared to the temperature effect on the fracture strength and fracture strain, the strain rate effect is not significant. The results from the NLE theoretical model agree reasonably well with the MD data.

B. Graphene with slits

As shown in Sec. IV A, pristine monolayer graphene has excellent mechanical properties. However, during fabrication of graphene, defects cannot be fully prevented.[34] Defects typically cause degradation of the mechanical properties. To systematically investigate the effect of defects—especially slits in nanoscale—on the strength and stiffness of graphene, we investigate a 5 nm×5 nm squarelike graphene sheet with a slit shown in Fig. 5. After initial equilibration of the structure, a strain rate of 0.0005 ps^{-1} is applied along the armchair direction to perform the uniaxial tensile test. When fracture occurs, the bonds break continuously, along the slit direction starting from the slit tip, till the graphene structure falls apart. The length of the slit ($2L=2\rho+nL_0$ with n=1,2,3…) and the radius of the tip $\rho=\sqrt{3}/2L_0$ are also shown in the figure. $2w$=5 nm is the finite width of the graphene monolayer along the slit direction. Figure 6 shows the variation in the fracture strength as a function of slit semilength at temperatures of 300 and 1200 K. The analytical approximations from Eq. (11) with σ_r from Eq. (8) are also shown for comparison. Clearly, the fracture strength de-

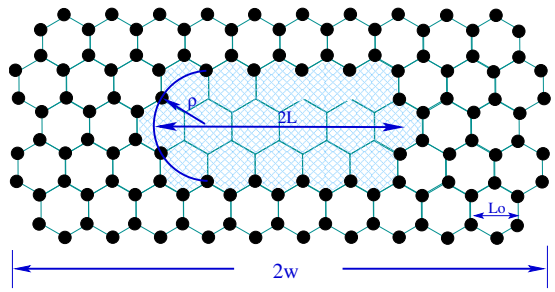

FIG. 5. (Color online) The atomic-scale slit structure of graphene for mode I loading. The definitions of various parameters in Eq. (11) are shown in the diagram.

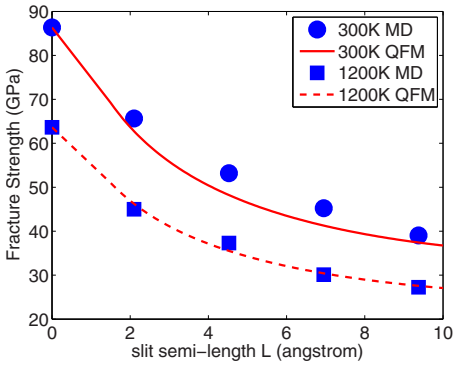

FIG. 6. (Color online) Fracture strength σ_f as a function of slit semilength L for a cracked graphene monolayer, uniaxially loaded along the armchair direction. MD data (symbols) and the theoretical approximations (lines) are shown at 300 and 1200 K.

creases with the increase in slit length. The theoretical results match reasonably well with the MD results. The variation in the normalized fracture strength with the slit semilength is shown in Fig. 7. Comparison with the published numerical data for other materials and structures, such as Si, SiC, C, Ge,[35] and single wall CNTs[21] is also shown. While all the materials and structures follow the same variation with slit semilength, graphene shows slightly higher fracture strength and can be considered as one of the strongest materials.

V. CONCLUSION

In this paper, by using MD simulations, we investigated the effects of temperature, strain rate, and defects on the mechanical properties of monolayer graphene by performing the uniaxial tensile test along the armchair direction. We found that the variation in Young's modulus is relatively small (within a 10% range) for the pristine graphene monolayer when temperature varies between 300 and 2400 K. Compared to the strain rate, temperature, and defects have significant effect on the fracture strength of monolayer graphene. The fracture strength at 2400 K is about 40% of its value at room temperature (300 K). We have also shown that the results from the NLE theory on fracture strength as a function of temperature, strain rate, and slit length match reasonably with MD data. By comparing the strength of graphene with experimental and simulation data of other ultrastrong nanomaterials/nanostructures, we can conclude that graphene is an exceptionally strong material.

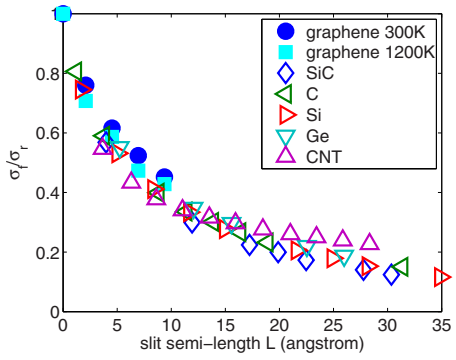

FIG. 7. (Color online) Comparison of fracture strength σ_f normalized with respect to the ideal strength σ_r as a function of slit semilength L for graphene at two different temperatures with values reported in literature for SiC, C, Si, and Ge samples [all uniaxially loaded along the [111] direction (Ref. 35)] and CNT [uniaxially loaded along the armchair direction (Ref. 14)].

ACKNOWLEDGMENTS

This work is supported by the National Science Foundation through Grant Nos. 0810294 and 0941497.

[1] M.-F. Yu, O. Lourie, M. J. Dyer, K. Moloni, T. F. Kelly, and R. S. Ruoff, Science **287**, 637 (2000).
[2] G. Dereli and B. Sungu, Phys. Rev. B **75**, 184104 (2007).
[3] Y. R. Jeng, P. C. Tsai, and T. H. Fang, Phys. Rev. B **71**, 085411 (2005).
[4] Z. G. Wang, X. T. Zu, F. Gao, and W. J. Weber, Eur. Phys. J. B **61**, 413 (2008).
[5] E. W. Wong, P. E. Sheehan, and C. M. Lieber, Science **277**, 1971 (1997).
[6] Z. G. Wang, X. T. Zu, F. Gao, and W. J. Weber, Phys. Rev. B **77**, 224113 (2008).
[7] H. Iwanaga and C. Kawai, J. Am. Ceram. Soc. **81**, 773 (1998).
[8] B. Wu, A. Heidelberg, and J. J. Boland, Nature Mater. **4**, 525 (2005).
[9] H. S. Park and J. A. Zimmerman, Phys. Rev. B **72**, 054106 (2005).
[10] S. K. R. S. Sankaranarayanan, V. R. Bhethanabotla, and B. Joseph, Phys. Rev. B **76**, 134117 (2007).
[11] G. Brambilla and D. N. Payne, Nano Lett. **9**, 831 (2009).
[12] C. Wei, K. Cho, and D. Srivastava, Phys. Rev. B **67**, 115407 (2003).
[13] M. Sammalkorpi, A. Krasheninnikov, A. Kuronen, K. Nordlund, and K. Kaski, Phys. Rev. B **70**, 245416 (2004).
[14] S. Zhang, S. L. Mielke, R. Khare, D. Troya, R. S. Ruoff, G. C. Schatz, and T. Belytschko, Phys. Rev. B **71**, 115403 (2005).
[15] K. S. Novoselov, A. K. Geim, S. V. Morozov, D. Jiang, Y. Zhang, S. V. Dubonos, I. V. Grigorieva, and A. A. Firsov, Science **306**, 666 (2004).
[16] A. K. Geim and K. S. Novoselov, Nature Mater. **6**, 183 (2007).
[17] Y. Zhang, T.-T. Tang, C. Girit, Z. Hao, M. C. Martin, A. Zettl, M. F. Crommie, Y. R. Shen, and F. Wang, Nature (London) **459**, 820 (2009).
[18] C. Lee, X. Wei, J. W. Kysar, and J. Hone, Science **321**, 385 (2008).
[19] F. Liu, P. Ming, and J. Li, Phys. Rev. B **76**, 064120 (2007).
[20] H. Zhao, K. Min, and N. R. Aluru, Nano Lett. **9**, 3012 (2009).
[21] R. Khare, S. L. Mielke, J. T. Paci, S. Zhang, R. Ballarini, G. C. Schatz, and T. Belytschko, Phys. Rev. B **75**, 075412 (2007).
[22] S. N. Zhurkov, Int. J. Fract. Mech. **1**, 311 (1965).
[23] G. Halsey, H. J. White, and H. Eyring, Text. Res. J. **15**, 295 (1945).
[24] S. Arrhenius, Z. Phys. Chem. **4**, 226 (1889).
[25] J. Bailey, The Glass Industry **20**, 21 (1939).
[26] A. I. Slutsker, V. I. Betekhtin, J. C. Lee, D. Yusupov, A. G. Kadomtsev, and O. V. Amosova, Acta Mater. **52**, 2733 (2004).
[27] A. A. Griffith, Philos. Trans. R. Soc. London, Ser. A **221**, 163 (1920).
[28] N. M. Pugno and R. S. Ruoff, Philos. Mag. **84**, 2829 (2004).
[29] N. Pugno, A. Carpinteri, M. Ippolito, A. Mattoni, and L. Colombo, Eng. Fract. Mech. **75**, 1794 (2008).
[30] T. L. Anderson, *Fracture Mechanics: Fundamentals and Applications*, 2nd ed. (CRC, Boca Raton, 1995).
[31] S. Plimpton, J. Comput. Phys. **117**, 1 (1995).
[32] S. J. Stuart, A. B. Tutein, and J. A. Harrison, J. Chem. Phys. **112**, 6472 (2000).
[33] O. A. Shenderova, D. W. Brenner, A. Omeltchenko, X. Su, and L. H. Yang, Phys. Rev. B **61**, 3877 (2000).
[34] A. Hashimoto, K. Suenaga, A. Gloter, K. Urita, and S. Iijima, Nature (London) **430**, 870 (2004).
[35] A. Mattoni, M. Ippolito, and L. Colombo, Phys. Rev. B **76**, 224103 (2007).